UV-laser Treatment in the Nanodomain: Forming of Organic Nanofibers

F. Balzer[*], R. Frese[**], M. Madsen[**], K. Thilsing-Hansen[**] and H.-G. Rubahn[**]

[*]*Institut für Physik/ASP, Humboldt-Universität zu Berlin, D-12489 Berlin, Germany*
[**] *Mads Clausen Institute,NanoSYD,*
University of Southern Denmark, DK-6400 Sønderborg, Denmark
E-mail: rubahn@mci.sdu.dk

Nanofibers grown in a sophisticated surface self assembly process from organic molecules are important key elements for future nanoscaled optoelectronic devices. They might serve both as passive elements such as waveguides and as active elements such as nanoscaled light sources or nanolasers. For both applications, structuring of the nanofibers by defined cutting is very important. However, as with all surface grown nanoaggregates, this is a difficult task when applying conventional mechanical cutting methods. In this article we show that excimer laser treatment at 193 nm provides a valuable alternative. We find that irradiation at a fluence of 100 mJ/cm^2 removes the fibers completely without damaging the growth substrate mica. In addition, the fibers can be cut in any orientation relative to their long axes. Ablation and cutting work even better for nanofibers transferred onto other substrate surfaces such as glass. We investigate the quality of the ablation process in terms of nanofiber bleaching, substrate destruction and steepness of cutting by atomic force as well as fluorescence microscopy. It is shown that the imaging focus position has a critical influence on the steepness, with a so far limiting value of 400 nm.

DOI: 10.2961/jlmn.2006.03.0024
Keywords: Excimer laser ablation, organic nanofibers, laser cutting

1. Introduction

It has been demonstrated thoroughly that organic molecules such as phenylenes can form long, quasi-single crystalline aggregates ("nanofibers" or "nanoneedles") of parallel to the surface oriented molecules on cleaved muscovite mica upon vapor deposition (organic molecular beam epitaxy, OMBE). Phenylenes of that kind are rodlike molecules of usually between four and six benzene rings, which emit polarized blue light after UV excitation below 400 nm. Via functionalization with, e.g., methyl oxide or chlorine end groups the emission spectra can be significantly modified. The surface grown nanofibers are all mutually parallel oriented because of strong electric dipole fields on the mica surface and a quasi heteroepitaxial relationship between adsorbate and substrate [1,2]. That way domains of parallel aggregates up to square centimeter size are grown.

Whereas individual aggregates can reach lengths of several hundred micrometers, their widths and heights are a few ten to a few hundred nanometers as measured by atomic force microscopy (AFM). Widths, heights, lengths as well as the number density of the aggregates on the surface can be controlled nearly independently of each other by choosing appropriate process parameters during deposition in vacuum.

Organic nanofibers are of special interest for the generation of single- or multi-fiber optoelectronic devices such as evanescent wave biosensors or organic nanolasers since waveguiding along para-hexaphenyl based fibers [3] as well as lasing [4] have been demonstrated recently. However, the application potential of nanofibers for micro- and nanooptical devices relies heavily on the coupling efficiency of external light. Especially the use of the fibers as interconnecting optical elements asks for light transfer through the endfaces of the fibers. Assembling an organic nanolaser from a single fiber requires well defined endfaces, too, which may eventually be covered with a thin metallic or dielectric layer to build a resonator structure.

The main problem in cutting or shaping the endfaces of the fibers is their extremely small dimensions with heights around 50 nm and widths of the order of several hundred nanometers. These exclude any direct mechanical cutting methods and point to optical cutting methods.

Micro fabrication by laser ablation has become a strong and flexible tool for the generation of components or devices for a variety of applications in micro-electronics, micro-mechanics, micro-fluidics, and micro-optics. In many cases the ablative removal of material is applied to fabricate holes, channels or three dimensionally shaped surfaces. Micro lenses, waveguides, and gratings are examples for optical elements, which can be fabricated this way.

Generally, the quality of the generated structures increases when reducing the ablating laser wavelength. Besides providing higher optical resolution, this is mainly due to stronger absorption leading to a more confined interaction volume. Thus transparent polymers like PMMA or polycarbonate can be processed with much higher precision at a laser wavelength of 193 nm compared to, e.g., 308 nm. This should also be true for the phenylenes that the present nanofibers are made of. However, at a wavelength of 193 nm even substrate materials that are transparent in the visible spectral range like glass, ceramics or mica start to absorb strongly, so that their ablation- or damage thresholds

are easily reached. In the case of removing a film or nano-aggregate from a substrate, this leads to the existence of a sometimes narrow "processing window", where the fluence is sufficient to ablate the layer, but not so high that the substrate is damaged.

Recently we have found ways to transfer organic nanofibers from their growth substrate to any arbitrary substrate. This provides us with the possibility to perform UV-laser (193 nm) ablation and cutting experiments on organic nanofibers supported on various absorbing and non-absorbing substrates. In this paper we demonstrate that we are able to remove and to cut the fibers without damaging the substrate surface. We also find optimum parameters for cutting the end faces at a steep angle.

2. Experimental

Organic nanofibers from para-hexaphenyl (p-6P) have been grown on cleaved muscovite mica in an OMBE-machine as detailed previously [2]. After growth they have either been used directly on the growth substrate mica or they have been transferred to another substrate such as glass via a wet transfer process [5].

Ablation was performed with an ArF excimer laser emitting at 193 nm in a mask projection set-up. The masks were imaged with 25× demagnification (Schwarzschild reflective objective, numerical aperture 0.4) on the sample resulting in irradiation spots of 100 × 100 μm^2 and 10 × 6 μm^2, respectively. The fluence was controlled using a variable dielectric attenuator, measuring the pulse energy by a pyroelectric Joulemeter. As masks we have used crossed razor blades of various distances.

3. Results and discussion

Nanofibers as grown

Due to the crystal growth mode the end faces of the as grown nanofibers can be very steep, leading in fact to strongly enhanced optical radiation from these faces. The steepness is demonstrated in Fig.1 by an atomic force microscope (AFM) image of the tip of such a nanofiber.

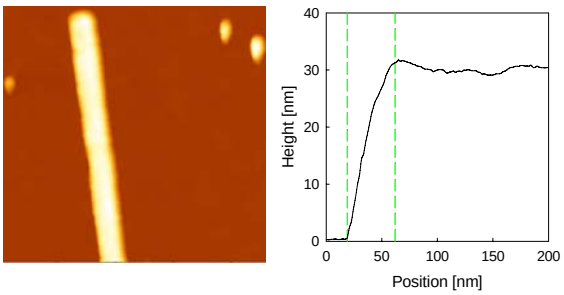

Fig. 1 AFM image (900 × 900 nm^2) of the tip of an "as grown" p-6P nanofiber; height scale 40 nm. On the right-hand-side a section across the end of the fiber is presented, showing a rather steep decrease within less than 50 nm (vertical dashed lines), even without deconvolution of the image with the AFM tip shape. Note that this image represents nanofibers with the steepest endfaces - many of them are less perfect.

Within less than 50 nm the fiber height changes from its maximum value to the surface plane. We note that this image has not been deconvoluted from the AFM tip shape, which obviously restricts the possible morphological resolution. Hence the 'real' steepness of the fibers is even better than shown on this image and just given by the order to the phenylene crystal.

In this specific image the fiber end is also nearly perpendicular to the long axis of the aggregate. Due to the fibers single crystalline nature this is not necessarily the case for all fibers. Facets with various angles may occur as well as rounded endfaces. At present we are not aware of any way to control the orientation or steepness of the end faces of the fibers via direct manipulation of the growth process. Hence the end faces have to be cut on purpose afterwards.

Slicing of nanofibers

An appropriate way of manipulating single nanoscaled objects obviously is to use a tool that has nanoscaled dimensions such as the tip of the atomic force microscope (AFM). Figure 2 shows para-hexaphenyl fibers on muscovite mica, which have been sliced by an AFM tip in intermittent contact mode by lowering the set point continuously during scanning from the lower right to the upper left.

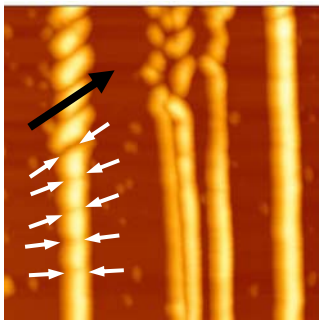

Fig. 2 AFM image (2 × 2 μm^2) of nanofibers, cut by the tip of an atomic force microscope in intermittent contact mode (JPK NanoWizard). The height scale of the image is 34 nm. The black arrow denotes the cutting direction, the white arrows emphasize the directions of the cuts within the needle on the left.

A section through a cut fiber reveals that the depth cuts can, but do not have to go down to the substrate, depending on the force exerted on the fiber. The periodicity of the cuts in this case is 200 nm, but can be choosen almost arbitrarily down to 50 nm. The (2 × 2) μm^2 AFM image of a scratched area demonstrates that some slices have been bent and rotated by the scratching process. The arrows in Fig. 2 denote the directions of the scratches, which for the a few nanometer deep scratches are not parallel to the scratch direction (120°, black single-headed arrow), but are almost perpendicular to the long needle axis (i.e. the cutting angle is close to 90°, c.f. the analysis in Fig. 3).

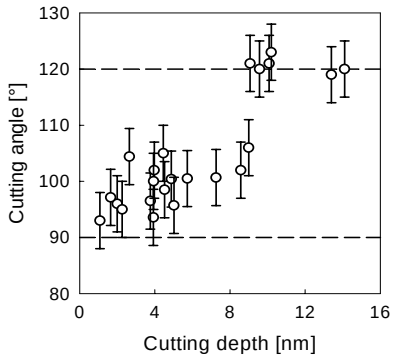

Fig. 3 Analysis of the cutting angles as a function of cutting depth for fixed angle of the AFM tip with respect to the nanofiber axis. The two dashed horizontal lines denote the cutting angle (120°) and the angle perpendicular to the long fiber axis (90°).

As shown also in Fig. 3 only for scratches as deep as at least 10 nm the direction of the cuts is along the scratch direction. For shallower scratches the scratch direction is closer to the short needle axis (i.e. exhibit a cutting angle close to 90°). A possible reason for this "natural" cutting direction is the orientation of the molecules within the lattice of a single fiber and thus the anisotropic surface tension.

Fluorescence microscope images of an AFM-scratched area are depicted in Fig. 4. The double-headed arrow denotes the direction of the needles. On the right-hand-side a polarizer has been placed in front of the CCD camera so that the transmission direction is parallel to the long fiber axis. Almost no fluorescence light from the fibers that have not been touched by the AFM tip passes the polarizer, whereas from the scratched ones significantly more light reaches the camera.

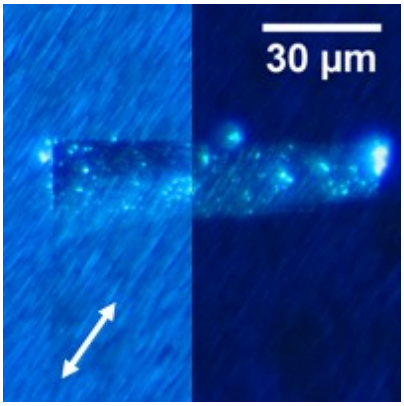

Fig. 4 Epifluorescence microscopy images of an AFM scratched area in a nanofiber sample. Scratching direction is the same as for Fig. 2. On the right-hand side only light polarized along the fiber direction (white arrow) reaches the CCD camera.

These results indicate a possible way for obtaining sub-hundred nanometer structures like, e.g., a Bragg grating on a number of parallel needles. However, slicing and cutting the fibers mechanically is a tedious process and disturbs the favorable optical properties of the fibers, i.e. the emission of polarized light after UV excitation, due to mechanical stress during the cutting process, Fig. 2.

Laser-induced cutting

As a first attempt to a more gentle, photonic cutting approach, we have used UV light from a tripled Nd-YAG laser, slightly focused onto a nanofiber coated mica sample (Fig. 5).

As seen from the displayed epifluorescence microscopy image, the 355 nm laser results in ablation of the nanofibers at fluences of around 0.1 mJ/cm^2. However, at the border of the laser spot, the nanofibers are molten and no sharp contours appear. Also, we observe bleaching of the nanofibers in the close neighborhood of the ablated area.

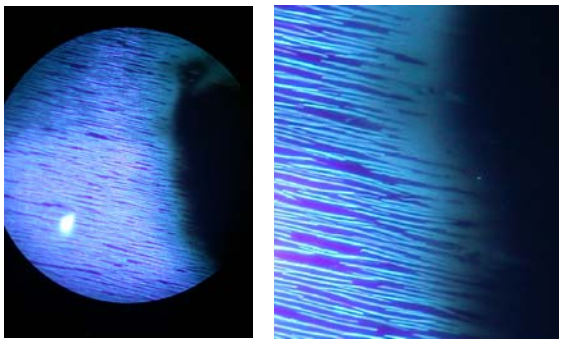

Fig. 5 Epifluorescence image of an array of organic nanofibers on mica irradiated with a single pulse of 355 nm UV laser light at 0.1 mJ/cm^2. The right-hand-side is a blow-up of the left-hand-side.

This is a typical signature for a thermal ablation process, accompanied by surface melting. This deteriorating effect should be avoidable using cold ablation as provided by deep UV, excimer laser light. We note in passing that exactly the same effect has also been observed for nanofibers on glass, irradiated with 355 nm UV light. Hence as concerns the quality of cutting of nanofibers there is no substrate influence (glass vs. mica) observable.

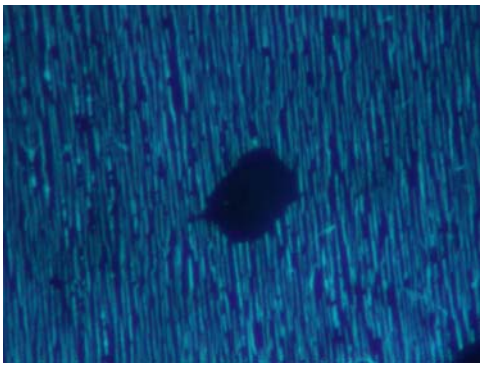

Fig. 6 Epifluorescence image of an array of organic nanofibers on glass, irradiated with a single pulse of 193 nm UV laser light (200 mJ/cm^2). The ablated area has a size of 10×6 µm^2.

Fig. 6 shows a micron-scaled ablated area in an organic nanofiber array, induced by UV laser light. The nanofibers seem to be perfectly removed with no obvious damage of the underlying substrate surface at fleunces above 100 mJ/cm^2. Also, there is no apparent bleaching of the nanofibers around the ablation hole. However, as seen in the corresponding AFM image (Fig.7), the glass surface is molten by the UV laser interaction, showing a ripple structure.

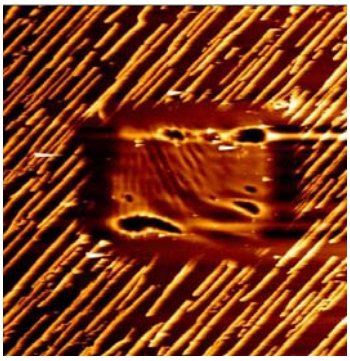

Fig. 7 AFM image (20 × 20 μm^2) of the ablated area of nanofibers shown in Fig. 6. Obviously, the glass surface is molten and shows a ripple structure.

A close up of two cut nanofibers (Fig. 8) reveals a steepness of the cut of the order of 800 nm. For comparison, a naturally occurring break in the nanofiber shows essentially the resolution limit of the AFM tip and the best possible, naturally occurring steepness of an endface, c.f. Fig.1.

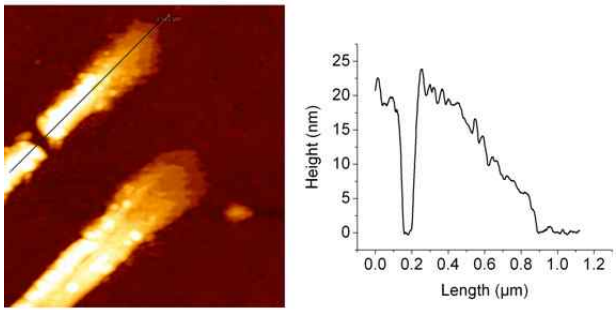

Fig. 8 AFM image (1.2 × 1.2 μm^2) of two cut nanofibers from Fig. 7. On the right-hand-side the section along one of the fibers demonstrates the rather smooth descent of a cut endface.

Optimizing the ablation can be performed either via changing the excimer laser fluence or the focusing of the laser.

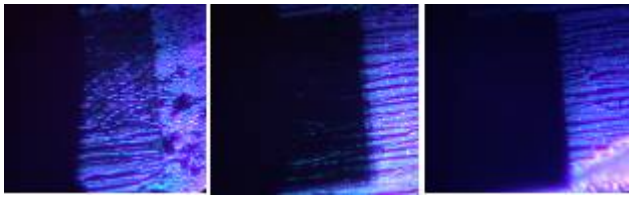

Fig. 9 Epifluorescence micrographs (100 × 100 μm^2) of hexaphenyl nanofibers on mica, irradiated by single UV pulses (193 nm) with 60 mJ/cm^2 (left-hand-side), 80 mJ/cm^2 (middle) and 100 mJ/cm^2 (right-hand-side).

Fluorescence images of samples irradiated with different fluences by single UV laser shots are presented in Fig. 9. As seen, at 100 mJ/cm^2 a clear ablation pattern is obtained. Again, there are no significant bleaching effects on the remaining fiber pieces. A direct comparison of ablated and non-ablated areas with the maximum possible optical resolution is shown in Fig. 10. Whereas the border region of the nanofibers is undefined preceding the ablation process, it becomes straightened after the ablation. There is no hint for a melting of the nanofibers and only very weak bleaching at the very ends of the fibers.

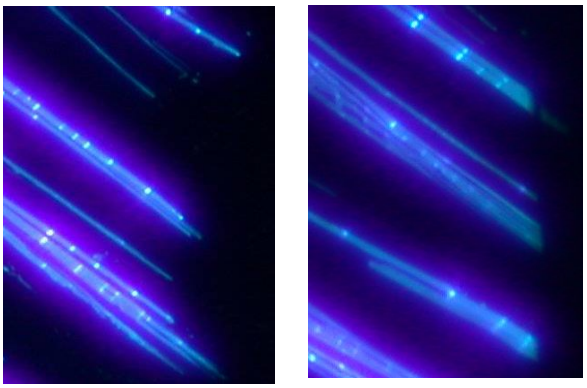

Fig. 10 Epifluorescence micrographs (100 × 60 μm^2) of end sections of hexaphenyl nanofibers on mica, not irradiated (left-hand-side) and irradiated with a mask at the very right-hand edge by two 100 mJ/cm^2 UV pulses (193 nm). The fibers are clearly cut on the right-hand-side.

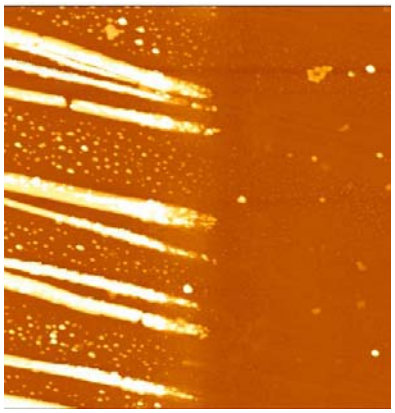

Fig. 11 AFM image (7 × 7 μm^2) of an array of organic nanofibers irradiated with 193 nm UV laser light. Note that the ablated area has been cleaned not only from the nanofibers, but also from the small cluster in between them and from the wetting layer. This image in fact proofs the existence of such a layer.

A closer look at the border region separating ablated and non-ablated fiber parts is given in Fig. 11 with the help of an atomic force microscopy image. In between the fibers lots of small islands are located, which are remaining from the growth process of the needles. Apparently even these small p-6P aggregates are completely removed by the ablation process and the fiber ends are all lined up and possess a predefined angle of 67° with respect to the fibers long

axes. This angle could be adjusted easily, e.g., to obtain Brewster angle cut fibers.

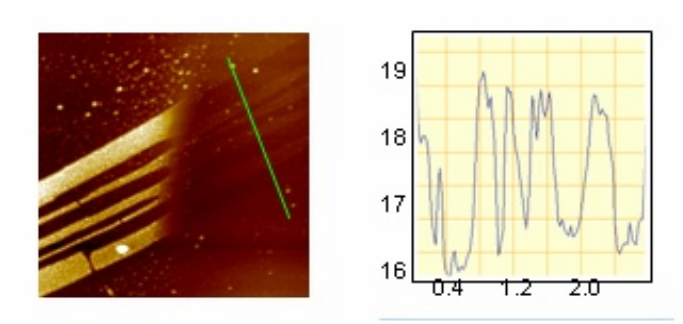

Fig. 12 AFM image (6.4 × 6.4 μm^2) of an array of organic nanofibers irradiated with 193 nm UV laser light. In this image the wetting layer has only been removed at the places where the nanofibers have been grown. The line scan on the right-hand-side (x-axis in μm and y-axis in nm) indicates that the wetting layer, consisting possibly of several layers of lying molecules, is about 1 - 4 nm tall.

Within the ablated area often a shadow image of the prior nanoneedle morphology remains, Fig. 12. Shadows of the fibers are in fact *below* the surface level. Obviously, either a few layers of mica (step height 1 nm) have selectively been ablated together with the fibers, or the area in between the fibers is covered with material, which has a higher ablation threshold than the fibers. From growth studies of p-6P on muscovite mica it is known that the fiber growth follows a Stranski-Krastanov growth mode, i.e. first a wetting layer from lying molecules forms, and after that fibers agglomerate from initially formed p-6P islands [6]. The binding energy of the wetting layer to the mica substrate is larger than the binding energy of the needles to the substrate [7]. Therefore an intriguing explanation for the shadow image might be the wetting layer, which in between the fibers is not removed by the ablation process because of its higher binding energy.

Besides optimizing the power of the ablating laser, optimum contrast of the projected image in the surface plane is of course most important for obtaining as steep as possible edge profiles. Figures 13 and 14 show how a micrometric change in the plane of the mask image with respect to the nanofiber surface plane affects the ablation profile. Here, the focus position '0' is an arbitrary value, whereas the movement from this value is given in micrometers. Hence '0' is not an indication of sharpest focus. From figures 13 and 14 we deduce that the sharpest focus is reached in between -30 and -45 micrometer away from our arbitrary zeropoint.

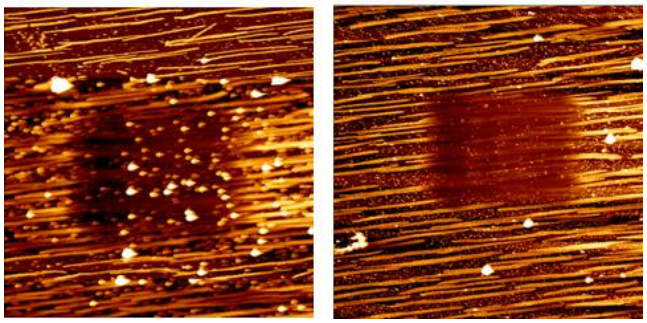

Fig. 13 AFM image (15 × 15 μm^2) of an array of organic nanofibers on glass, irradiated with 193 nm UV laser light at focus positions 0 and -15 μm. The height scale of both images is 24 nm.

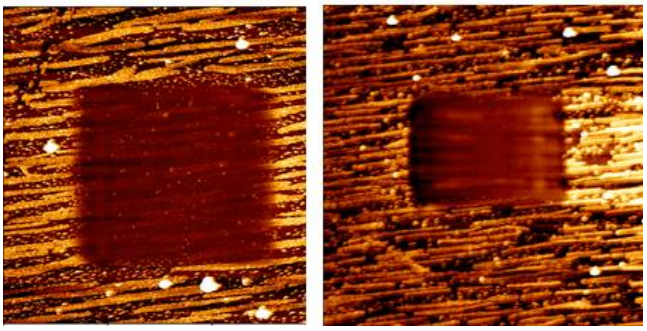

Fig. 14 Same as Fig.13, but for focus positions -30 μm and -45 μm.

Obviously at sharpest focus the ablation hole becomes better defined and especially the nanofiber end faces are cut under a steeper angle. This is quantified by height profiles across the end faces in Fig.15.

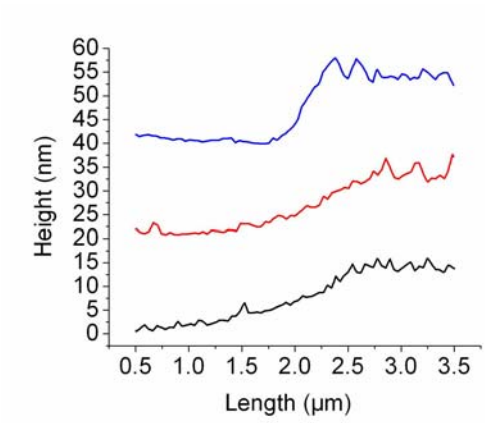

Fig. 15 Measured line profiles for cut nanofibers at focus positions -45, -30 and -15 μm according to Fig. 13 and Fig. 14. At optimum position (uppermost curve) a steepness of 400 nm is obtained.

Although laser ablation is well suited to write structures with a couple of hundred nanometers feature size, subhun-

dred nanometer resolution has not been achieved, yet. Multiphoton processes as well as reducing the pulse length from nanoseconds to pico- or even femtoseconds might overcome these problems in the future.

4. Conclusions

Organic nanoaggregates grown from para-hexaphenyl molecules under well-defined growth conditions in a high vacuum apparatus are versatile test objects for possible new integrated photonic elements. One of the main obstacles before implementing them in more complex devices as, e.g., waveguides, frequency doublers or lasing elements, is the coupling of light from or to them. In the present paper we have demonstrated that para-hexaphenyl nanofibers can be removed from a muscovite mica surface and from glass, and that they can be cut at arbitrary angles using 193 nm UV laser light pulses. We have found a nanometric definition of the lateral angle of the fiber ends (i.e. their angles in the surface plane), which can be arbitrarily set to any value. Debris from the ablation process, which readsorbs onto the nanofibers, does not deteriorate the waveguiding or frequency doubling properties and as such can be neglected.

As for the horizontal cutting angle definition up to now a minimum width of 300 – 400 nm for the cutting region has been obtained. Whether there is a deteriorating effect of this weak definition on the effective acceptance angles of the nanofibers still has to be investigated. However, as demonstrated by some of the "as grown" fibers, the vertical edge steepness could be improved. Possible routes to improvement are tilt-angle projection, pre-adsorption of an ultrathin light-absorbing layer, immersion-medium enhanced projection or encapsulation of the nanofibers.

Acknowledgments

We are grateful to the Danish research agencies STVF and SNF (FNU) for funding this work.

References

[1] F. Balzer and H.-G. Rubahn: Appl. Phys. Lett., 79, (2001) 3860.
[2] F. Balzer and H.-G. Rubahn: Adv. Funct. Mat., 15, (2005) 17.
[3] F. Balzer, V.G. Bordo, A.C. Simonsen, and H.-G. Rubahn: Appl. Phys. Lett., 82, (2003) 10.
[4] F. Quochi, F. Cordella, A. Mura, G. Bongiovanni, F. Balzer, and H.-G. Rubahn: Appl. Phys. Lett., 88, (2006) 041106.
[5] J. Brewer, C. Maibohm, L. Jozefowski, L. Bagatolli, and H.-G. Rubahn: Nanotechnology, 16 (2005) 2396.
[6] F. Balzer and H.-G. Rubahn: Surface Science, 548, (2004) 170.
[7] C. Teichert, G. Hlawacek, A.Y. Andreev, H. Sitter, P. Frank, A. Winkler, and N.S. Sariciftci: Appl. Phys. A, 82, (2006) 665.

(Received: May 16, 2006, Accepted: December 6, 2006)